Published in final edited form as:
Am J Trop Med Hyg. 2008 November ; 79(5): 760–767.

A Magnetic Resonance Imaging Study of Intestinal Dilation in *Trypanosoma cruzi*–infected Mice Deficient in Nitric Oxide Synthase

Lars Ny,
Department of Oncology, Sahlgrenska University Hospital, SE-413 45 Göteborg, Sweden

Hua Li,
Department of Physiology and Biophysics, Albert Einstein College of Medicine, Bronx, NY 10461

Shankar Mukherjee,
Department of Pathology, Albert Einstein College of Medicine, Bronx, NY 10461

Katarina Persson,
School of Pure and Applied Natural Sciences, University of Kalmar, SE-391 82 Kalmar, Sweden

Bo Holmqvist,
Department of Pathology, Lund University Hospital, SE-221 85 Lund, Sweden

Dazhi Zhao,
Department of Pathology, Albert Einstein College of Medicine, Bronx, NY 10461

Vitaliy Shtutin,
Department of Pathology, Albert Einstein College of Medicine, Bronx, NY 10461

Huan Huang,
Department of Pathology, Albert Einstein College of Medicine, Bronx, NY 10461

Louis M. Weiss,
Departments of Pathology and Medicine, Albert Einstein College of Medicine, Bronx, NY 10461

Fabiana S. Machado,
Division of Molecular Immunology, Cincinnati Children's Hospital Medical Center, Cincinnati, OH and the Department of Biochemistry and Immunology, Federal University of Minas Gerais, Belo Horizonte, Brazil

Stephen M. Factor,
Departments Pathology and Medicine, Albert Einstein College of Medicine, Bronx, NY 10461

John Chan,
Departments of Microbiology and Immunology and Medicine, Albert Einstein College of Medicine, Bronx, NY 10461

Herbert B. Tanowitz*, and
Departments of Pathology and Medicine, Albert Einstein College of Medicine, Bronx, NY 10461

*Address correspondence to Herbert B. Tanowitz, Departments of Pathology and Medicine, Albert Einstein College of Medicine, 1300 Morris Park Avenue, Bronx, NY 10461. E-mail: E-mail: tanowitz@aecom.yu.
Reprint requests: Herbert B. Tanowitz, Department of Pathology, Albert Einstein College of Medicine, 1300 Morris Park Avenue, Bronx, NY 10461, E-mail: tanowitz@aecom.yu.edu.

Linda A. Jelicks
Department of Physiology and Biophysics, Albert Einstein College of Medicine, Bronx, NY 10461

Abstract

Infection with *Trypanosoma cruzi* causes megasyndromes of the gastrointestinal (GI) tract. We used magnetic resonance imaging (MRI) to monitor alterations in the GI tract of *T. cruzi*–infected mice, and to assess the role of nitric oxide (NO) in the development of intestinal dilation. Brazil strain–infected C57BL/6 wild-type (WT) mice exhibited dilatation of the intestines by 30 days post-infection. Average intestine lumen diameter increased by 72%. Levels of intestinal NO synthase (NOS) isoforms, NOS2 and NOS3, were elevated in infected WT mice. Inflammation and ganglionitis were observed in all infected mice. Intestinal dilation was observed in infected WT, NOS1, NOS2, and NOS3 null mice. This study demonstrates that MRI is a useful tool to monitor intestinal dilation in living mice and that these alterations may begin during acute infection. Furthermore, our data strongly suggests that NO may not be the sole contributor to intestinal dysfunction resulting from this infection.

INTRODUCTION

Our laboratory pioneered the use of imaging of mice in evaluating the pathogenesis of *Trypanosoma cruzi* infection in real time. For example, we used echocardiography and magnetic resonance imaging (MRI) in our studies on the evolution of *T. cruzi*-induced heart disease in a mouse model. The MRI also provides excellent soft tissue contrast and resolution without radiation exposure, making it an attractive technology for studies of the gastrointestinal (GI) tract and urinary bladder.[1,2] In fact, MRI has been used to evaluate the GI tract and bladder noninvasively in humans.[3,4] The noninvasive nature of MRI makes it especially attractive for studying animal models of chronic diseases, such as Chagas disease. Using MRI, we previously observed enlarged urinary bladders in mice infected with *T. cruzi*.[5] To our knowledge, MRI has not been previously used in the evaluation of the GI tract in *T. cruzi* infected mice.

Acute *T. cruzi* infection is followed by a lifelong chronic phase. Ten to thirty percent of infected individuals develop chronic Chagas disease with progressive inflammatory destruction of heart, muscles, nerves, and gastrointestinal tract tissue. In endemic areas, chronic Chagas disease is the leading cause of cardiovascular death among patients 30 to 50 years of age. During the chronic stage of infection 7–10% of individuals develop megasyndromes that may involve any part of the GI tract, but mainly the esophagus and the colon.[6–8] Megasyndromes are associated with gastrointestinal motility disturbances in patients with Chagas disease.[9,10]

Mice exhibit many of the functional, pathologic, and immunologic alterations observed in human infection, including cardiomyopathy and mega-organ syndromes.[5,11–14] Mori and others[15] used x-ray methods to investigate GI tract abnormalities in *T. cruzi*–infected mice. In those mice intestinal transit was normal during acute infection, although delayed evacuation time was observed in the chronic phase. Another x-ray study of infected mice demonstrated swelling of the stomach and colon.[16] Histologic examination revealed extensive changes of the intestinal muscle layer and the loss of colonic folds and myoenteric plexus. More recently, de Oliveira and others[17] demonstrated decreased intestinal motility in *T. cruzi* (Y strain) infected Swiss Webster mice using charcoal.

Neuronal destruction of the enteric plexuses, observed in chagasic patients with megacolon, has been associated with increased activity of nitric oxide (NO), and neuronal nitric oxide synthase (NOS1) is reduced in individuals with megacolon.[18,19] During acute infection there is an upregulation of the expression of cytokines and inducible NO synthase (NOS2), which is thought to facilitate parasite killing via enhanced release of NO.[20–24] The NOS isoforms

play an important physiologic role in GI physiology,[25] and the availability of mice deficient in NOS isoforms has facilitated studies aimed at understanding the role of NO in physiologic functions. For example, mice lacking NOS1 exhibit gastric dilation and stasis, whereas mice lacking NOS2 are more sensitive to inflammatory damage, and NOS3 null mice develop high blood pressure.[26,27] Previously, we demonstrated that CD1 mice, acutely infected with the Brazil strain of *T. cruzi*, exhibited increased expression of NOS2, decreased expression of NOS1, reduced Ca^{2+}-dependent (NOS1 and NOS3) activity, and increased NOS2 activity in the GI tract.[28]

In the present study, we determined whether this novel MRI technique could be used to examine the GI tract in a mouse model, and then to investigate the role of the NOS and NO in the GI tract of *T. cruzi*–infected mice. NOS1, NOS2, and NOS3 null mice were infected and compared with wild-type (WT) mice (C57BL/6). Using this novel MRI technique we determined that dilation of the intestine was observed in infected mice whether WT or null. These observations suggest that there is no major contribution of NO to intestinal dilation in murine *T. cruzi* infection. Most importantly, this is the first study to clearly demonstrate the utility of MRI in the serial evaluation of the GI tract in *T. cruzi* infected mice.

MATERIALS AND METHODS

Parasitology and pathology

The Brazil strain of *T. cruzi* was maintained by serial passages in C3H/He mice (Jackson Laboratories, Bar Harbor, ME). NOS1, NOS2, and NOS3 null and C57BL/6 mice (WT) (Jackson Laboratories) were infected with 10^4 trypomastigotes ($N = 40$ per genotype). Parasitemia was determined at days 15, 21, and 26 days post infection (dpi). Mice were examined using non-invasive MRI, and the GI tract was assessed during acute infection, 30 dpi. The GI tract was re-evaluated during the chronic stage (60 dpi) in surviving mice. Tissue (obtained from a cohort of mice at 29 dpi) for histology was fixed in 4% buffered formalin and stained with hematoxylin-eosin (H&E). Cumulative mortality of the infected mice was calculated. These studies were approved by The Institutional Animal Care and Use Committee of the Albert Einstein College of Medicine.

Immunohistochemistry

Tissue was fixed for 4 hours in a 4 C solution of 4% formaldehyde in phosphate-buffered saline (PBS); pH 7.4, and rinsed in 15% sucrose in PBS. The tissue pieces were then frozen at −40° C in an isopentane solution and stored at −70°C. Cryostat sections were cut at a thickness of 8–10 μm and thaw-mounted onto chrome-alum coated slides as described previously.[29] The sections were incubated overnight with primary antisera against protein gene product 9.5 (PGP; 1:2000; raised in rabbit; UltraClone, Isle of Wight, UK). The sections were examined using an Olympus OMX60 (Center Valley, PA) system fluorescence microscope. In control experiments, no immunoreactivity could be detected in sections incubated in the absence of primary antisera.

Semi-quantitative RT-PCR

Total RNA was obtained from a small group of infected (29 dpi) and uninfected mouse colons by TRIZOL reagent (Invitrogen, Carlsbad, CA) as recommended by the manufacturer. Total RNA was further purified using the RNeasy midi kit (Qiagen, Valencia, CA) and measured twice in Nanodrop ND1000 spectrophotometer (Thermo Scientific, Wilmington, DE) before subjecting to reverse transcription–polymerase chain reaction (RT-PCR). One microgram of the purified RNA was used to amplify NOS messenger RNA (mRNA) isoforms using GeneAmp RNA PCR kit (Applied Biosystems, Foster City, CA). Briefly, the first strand complementary DNA (cDNA) synthesis was performed at room temperature for 10 minutes,

reverse transcribed at 42°C for 15 minutes using 2.5 μM oligo-dT^{16} primer and 2.5 units MuMLV RT, and denatured at 99°C for 5 minutes. The cDNAs were then amplified by PCR using 2.5 units of Ampli Taq DNA polymerase (Perkin-Elmer, Foster City, CA) and NOS 1, NOS 2, and NOS 3 primer pairs were obtained from R&D systems (Minneapolis, MN) using specific primer pair kits with the following cycle, single cycle at 94°C for 3 minutes, 30 cycles of denaturation at 94°C for 45 seconds, annealing at 55°C for 45 seconds, extension at 72°C for 30s with a final extension at 72°C for 10 minutes in thermal cycler (GeneAmp PCR System 2400, Perkin Elmer). The positive controls for NOS isoforms were amplified for 35 cycles using Platinum PCR supermix (Invitrogen, Carlsbad, CA) and primer pairs obtained from R&D system kits. We used the following primers for amplification of glyceraldehyde-3-phosphate dehydrogenase, as a housekeeping control gene, forward 5′-TGAAGGTCGGTGTGAACGGAT-3′, reverse 5′-CATGTAGGCCATGAGGTCCAC-3′. The PCR products were vacuum-dried and electrophoresed in 0.9% agarose gel containing ethidium bromide. The gel image was captured in FluorChem (Alpha Innotech), and the bands quantitated in Image J software (NIH, Bethesda, MD).

Magnetic resonance imaging

Mice were anesthetized with 1–2% isoflurane administered with a nose cone and were positioned in a 40-mm birdcage RF coil (RF-Sensors LLC, New York, NY). Images were acquired using a vertical 9.4 T wide bore General Electric Omega spectrometer (Fremont, CA) operating at a proton frequency of 400 MHz and equipped with 50-mm shielded gradients. The temperature within the gradient coils was maintained at 30°C with a Neslab water cooling/heating unit (Thermo Scientific, Newington, NH) to maintain body temperature during the imaging experiment. Slice selection was achieved with a 90° sinc pulse. A 51.2-mm field of view was used. Each 128 × 256 pixel image was interpolated to 256 × 256 pixels. There was no separation between image slices. An echo time of 18 ms and repetition time of 400 ms was used. After locating the GI tract a series of transverse, sagittal, and coronal images were acquired to delineate the entire intestine. Image data was transferred to a PC for offline processing using MRI analysis software running in MATLAB (The Math Works, Inc., Natick, MA) and intestinal lumen diameters were measured at the level of the kidneys. The MRI images were then converted to JPEG format using MATLAB. The consecutive images were then loaded into Amira software (Mercury Computer Systems, Chelms-ford, MA) sequentially as a single entity. After all the images from each individual plane were properly arranged in Amira, they were merged into a single entity for the three-dimensional reconstructions.

Statistics

The data are expressed as the standard error of the mean (SEM). When statistical differences between two means were determined, an unpaired Student's *t* test was performed and $P < 0.05$ was regarded as significant. When statistical analyses between means were performed, all values refer to different animals if not otherwise stated.

RESULTS

Parasitemia, mortality, and histology

Mean parasitemia (at 26 dpi) was highest (2×10^6) in infected NOS1 null compared with WT mice, NOS2, and NOS3 null mice (4×10^5). Cumulative mortality was the highest for NOS1 null mice (70% at 36 dpi, $N = 12$) and no mice in this cohort survived to a chronic time point (60 dpi). Mortality was also high for infected NOS3 null mice (60% at 36 dpi, $N = 20$), and the mean parasitemia was not significantly different from infected NOS2 null or WT mice. Cumulative mortality was lower for WT (46% at 36 dpi and 70% at 60 dpi, $N = 13$) and NOS2 null (13% at 36 dpi and 33% at 60 dpi, $N = 15$) mice. Because of the high mortality of the NOS1 and NOS3 null mice, most of the data was collected during acute infection.

At 30 dpi a small cohort of WT and NOS null mice were killed and tissue was dissected and examined. The stomach and duodenum of uninfected NOS1 null mice were enlarged. Inflammation in the esophagus, small intestine, and colon was present in all infected mice, and it was most intense in infected NOS2 null mice (Figure 1). There was inflammation of the ganglia (ganglionitis) in all infected mice. No obvious differences in PGP-immunoreactivities were observed between infected and uninfected mice independent of strain demonstrating an intact nerve supply (Figure 2).

NOS isoforms by RT-PCR

Expression of NOS isoforms in the NOS1, NOS2, and NOS3 null mice was evaluated by RT-PCR (Figure 3 and Figure 4). Infected NOS1 null mice exhibited increased expression of NOS2 and NOS3 in colon. The NOS2 null mice expressed elevated levels of NOS3 in colon regardless of their infection status. The RT-PCR demonstrated that infected NOS2 null mice exhibited increased expression of NOS1 in colon. In colonic tissue obtained from NOS3 null mice there was no significant difference in expression of NOS1 or NOS2 in infected compared with uninfected mice.

MRI evaluation

The MRI provides excellent soft tissue contrast and resolution making it an attractive non-invasive technology for studies of the GI tract. We performed multiple MRI studies of the infected and uninfected mice and reconstructed the GI tract. We observed that the GI tract of chronically infected WT mice was enlarged compared with uninfected control mice (Figure 5, compare panels A and B).

Because previous studies indicated the importance of NO and NOS isoforms in the pathogenesis of Chagas disease, we examined the GI tract of NOS null mice. The GI tract morphology of uninfected NOS2 null and uninfected NOS3 null mice was similar to that observed in uninfected WT mice. However, uninfected NOS1 null mice exhibit extremely enlarged stomachs and intestines, which increased after infection (data not shown). Acutely infected NOS2 and NOS3 null (Figure 6) mice also exhibited enlargement of the GI tract. The degree of intestinal dilation was evaluated by measuring lumen diameters of the intestinal loops at the level of the kidney in the different mouse groups at the acute and chronic stages of infection. None of the infected NOS1 null mice survived to the chronic stage, and only one NOS3 null mouse survived to the chronic stage. Comparison of the lumen diameters for the uninfected and infected mice is shown in Figure 7. Infection caused a significant increase in lumen diameter in all mouse groups, and the degree of dilation was similar in acute and chronic infected mice. The lumen diameter of uninfected NOS1 null mice was significantly larger than that of all other uninfected groups and; therefore, increased to a lesser extent (12%) than other groups (which increased 66–74%).

DISCUSSION

Our laboratory group has pioneered the use of imaging techniques in the serial evaluation of many aspects of morphologic and functional alterations in the cardiovascular system and urinary tract of *T. cruzi*–infected mice. The GI tract is an important target of infection of *T. cruzi*. The few studies in mouse models have relied on histopathologic studies that require the sacrifice of individual mice, thus it is not possible to conduct serial studies in individual mice. Here we obtained MRI data on infected and uninfected WT and NOS1, NOS2, and NOS3 null mice. The MRI results demonstrated enlargement of the GI tract of all infected mice regardless of genotype.

Increased expression of NOS3 was observed in the colonic tissue of infected NOS1 null mice. In the infected NOS1 null mouse, the high parasitemia and mortality was significantly increased compared with the infected WT mouse. To our knowledge, this is the first time this observation has been made. The reason for this is not clear. However, it may suggest that compensatory increased expression of NOS2 and NOS3 cannot compensate for deficiency of NOS1 during this infection. It is possible that infection in the setting of already compromised absorption of nutrients made these mice less able to mount an effective immune response. In a recent study, Li and others[30] observed that NOS1 is necessary for clearance of *Giardia lamblia* infection in mice. *Giardia*–infected NOS1 deficient mice exhibited higher numbers of parasites and prolonged infection. The NOS1 is involved in intestinal motility and NOS1 null mice exhibit reduced gastric emptying, which may be related to the prolonged *Giardia* infection in those mice.[30] Gastrointestinal motility disturbances have been observed in patients with Chagas disease and in mice infected with *T. cruzi*.[10,18] Interestingly, the present MRI and mortality results are consistent with the observations that loss of NOS1 was associated with more severe disease and increased mortality in a mouse model of colitis.[31]

Previous studies of the gut of humans and animals demonstrated increased NOS2 expression in disease states associated with inflammation, endotoxemia, and colitis. In rodents, NOS2 expression can be inhibited by treatment with NOS-inhibiting agents resulting in an augmented inflammatory response.[32] Induction of inflammation in NOS2 null mice results in an increased cellular response in comparison to WT mice.[33] Therefore, it has been suggested that NOS2 has a critical protective function to limit inflammation.

In experimental models of *T. cruzi* infection there is an increased NOS2 expression that is likely induced by increased synthesis of proinflammatory cytokines and it has been suggested that this has both beneficial and detrimental effects because NO limits the proliferation of the parasite, but contributes to myocardial dysfunction. We and others have demonstrated that lack of NOS2 does not reduce survival of infected mice, although high amounts of NO produced by NOS2 are important for microbial extinction in other diseases.[34–40]

The RT-PCR demonstrated increased expression of both NOS1 and NOS3 in the colon of infected NOS2 null mice. The lower mortality in these mice suggests that compensatory upregulation of NOS1 and NOS3 isoforms may provide some protection of the host from infection even though the GI tract morphology is altered to a similar degree in infected WT and NOS2 null mice, as demonstrated by MRI. Non-NO-dependant mediators and signaling pathways may also play a role. This was suggested by the results of Cummings and Tarleton demonstrating enhanced expression of TNFα, interleukin, and macrophage inflammatory protein 1α in NOS2 null mice.[35]

In the present report, infected NOS3 null mice displayed altered GI tract morphology and high mortality, but no significant change in expression of NOS1 and NOS2 in the colon as a result of infection, although infection typically results in induction of NOS2. Beck and others[31] observed that dextran sodium sulfate (DSS) treated NOS3 null mice also exhibited significantly less NOS2 induction than WT and NOS1 null mice. These results suggest that this pathway may be impaired in NOS3 null mice. Although the expression of the NOS1 and NOS2 isoforms were reduced in the colon, the infected NOS3 null mice exhibited a level of parasitemia comparable to that of the NOS2 null and WT mice and significantly lower than that of the NOS1 null mice, which also had high mortality. It is likely that infection induced damage to other organs contributes to the high mortality of the NOS3 null mice.

It is of interest that there was already MRI evidence of intestinal dilation during acute infection, which persisted into the chronic phase. Although dilation of the GI tract is not generally appreciated as a finding in acute human infection, it has been described as a consequence of

congenital Chagas disease.[41,42] Thus, our observations indicate that *T. cruzi* associated megasyndromes of the GI tract may appear much earlier than previously appreciated and suggests that individuals with Chagas disease at any stage should be evaluated for GI abnormalities. Furthermore, our observations using NOS null mice suggest that intestinal inflammation and dilation is not exclusively dependent on NO.

Most importantly, to our knowledge this is the first study that clearly demonstrates the use of MRI to serially monitor intestinal tract dilation in *T. cruzi*-infected mice obviating the need to perform pathologic studies requiring the sacrifice of the animals. This can be used in a variety of situations including immunologic and therapeutic studies. Coupled with echocardiography and MRI of the heart the application of these technologic advances will allow investigators to examine alterations in structure and function in murine Chagas disease in real-time.

Acknowledgments

Financial support: This study was supported by the Swedish Foundation for Strategic Research and grants from the United States National Institutes of Health (AI-062730 (LAJ), AHA SDG 0735252N (SM), AI052739, AI058893 (HH), and AI068538 (HBT).

REFERENCES

1. Tait P, Allison D. Imaging of the gastrointestinal tract. Drugs Today (Barc) 2001;37:533–557. [PubMed: 12743637]
2. Lomas DJ. Technical developments in bowel MRI. Eur Radiol 2003;13:1058–1071. [PubMed: 12695829]
3. Lawler LP, Fishman EK. Bladder imaging using multidetector row computed tomography, volume rendering, and magnetic resonance imaging. J Comput Assist Tomogr 2003;27:553–563. [PubMed: 12886144]
4. Bruel JM, Gallix B. Multidetector CT and MRI in diseases of the GI tract. J Radiol 2003;84:499–513. [PubMed: 12844073]
5. Boczko J, Tar M, Melman A, Jelicks LA, Wittner M, Factor SM, Zhao D, Hafron J, Weiss LM, Tanowitz HB, Christ GJ. *Trypanosoma cruzi* infection induced changes in the innervation, structure and function of the murine bladder. J Urol 2005;173:1784–1788. [PubMed: 15821587]
6. Kirchhoff LV. American trypanosomiasis Chagas disease. Gastroenterol Clin North Am 1996;25:517–533. [PubMed: 8863038]
7. Tanowitz HB, Kirchhoff LV, Simon D, Morris SA, Weiss LM, Wittner M. Chagas disease. Clin Microbiol Rev 1992;5:400–419. [PubMed: 1423218]
8. da Silveira AB, Lemos EM, Adad SJ, Correa-Oliveira R, Furness JB, D'Avila Reis D. Megacolon in Chagas disease: a study of inflammatory cells, enteric nerves, and glial cells. Hum Pathol 2007;38:1256–1264. [PubMed: 17490721]
9. Madrid AM, Quera R, Defilippi C, Defilippi C, Gil LC, Sapunar J, Henriques A. Gastrointestinal motility disturbances in Chagas disease. Rev Med Chil 2004;132:939–946. [PubMed: 15478295]
10. Madrid AM, Defilippi C. Disturbances of small intestinal motility in patients with chronic constipation. Rev Med Chil 2006;134:181–186. [PubMed: 16554925]
11. Scremin LH, Corbett CE, Laurenti MD, Nunes EV, Gama-Rodrigues JJ, Okumura M. Megabladder in experimental Chagas disease: pathological features of the bladder wall. Rev Hosp Clin Fac Med Sao Paulo 1999;54:43–46. [PubMed: 10513065]
12. Postan M, Cheever AW, Dvorak JA, McDaniel JP. A histopathological analysis of the course of myocarditis in C3H/He mice infected with *Trypanosoma cruzi* clone Sylvio-X10/4. Trans R Soc Trop Med Hyg 1986;80:50–55. [PubMed: 3726997]
13. Postan M, Bailey JJ, Dvorak JA, McDaniel JP, Pottala EW. Studies of *Trypanosoma cruzi* clones in inbred mice. III. Histopathological and electrocardiographical responses to chronic infection. Am J Trop Med Hyg 1987;37:541–549. [PubMed: 3318521]

14. De Rossell RA, Rodriguez AM, De Jesus R, Calcagno M, De Segnini ZM, Diaz S. Tripomastigotes de sangre y de cultivo celular de *Trypanosoma cruzi* Y.: II.—Patología de la enfermedad de Chagas en ratones Balb/c. Parasitol Dia 2000;24:79–87.
15. Mori T, Yoon HS, Iizuka FH, Myung JM, Sato HR, Silva MF, Okumura M. Intestinal transit and opaque enema study in chagasic mice. Rev Hosp Clin Fac Med Sao Paulo 2005;501:63–66.
16. Guillen-Pernia B, Lugo-Yarbuh A, Moreno E. Digestive tract dilation in mice infected with *Trypanosoma cruzi*. Invest Clin 2001;42:195–209. [PubMed: 11552508]
17. de Oliveira GM, de Melo Medeiros M, da Silva Batista W, Santana R, Araújo-Jorge TC, de Souza AP. Applicability of the use of charcoal for the evaluation of intestinal motility in a murine model of *Trypanosoma cruzi* infection. Parasitol Res 2008;102:747–750. [PubMed: 18163190]
18. Garcia SB, Paula JS, Giovannetti GS, Zenha F, Ramalho EM, Zucoloto S, Silva JS, Cunha FQ. Nitric oxide is involved in the lesions of the peripheral autonomic neurons observed in the acute phase of experimental *Trypanosoma cruzi* infection. Exp Parasit 1999;93:191–197. [PubMed: 10600444]
19. Ribeiro U Jr, Safatle-Ribeiro AV, Habr-Gama A, Gama-Rodrigues JJ, Sohn J, Reynolds JC. Effect of Chagas disease on nitric oxide-containing neurons in severely affected and unaffected intestine. Dis Colon Rectum 1998;41:1411–1417. [PubMed: 9823808]
20. Aliberti JC, Machado FS, Souto JT, Campanelli AP, Teixeira MM, Gazzinelli RT, Silva JS. β-Chemokines enhance parasite uptake and promote nitric oxide-dependent microbiostatic activity in murine inflammatory macrophages infected with *Trypanosoma cruzi*. Infect Immun 1999;67:4819–4826. [PubMed: 10456936]
21. Holscher C, Kohler G, Muller U, Mossmann H, Schaub GA, Brombacher F. Defective nitric oxide effector functions lead to extreme susceptibility of *Trypanosoma cruzi*-infected mice deficient in gamma interferon receptor or inducible nitric oxide synthase. Infect Immun 1998;66:1208–1215. [PubMed: 9488415]
22. Oswald IP, Wynn TA, Sher A, James SL. NO as an effector molecule of parasite killing: modulation of its synthesis by cytokines. Comp Biochem Physiol Pharmacol Toxicol Endocrinol 1994;108:11–18. [PubMed: 7520338]
23. Teixeira MM, Gazzinelli RT, Silva JS. Chemokines, inflammation and *Trypanosoma cruzi* infection. Trends Parasitol 2002;18:262–265. [PubMed: 12036740]
24. Vespa GN, Cunha FQ, Silva JS. Nitric oxide is involved in control of *Trypanosoma cruzi* induced parasitemia and directly kills the parasite *in vitro*. Infect Immun 1994;62:5177–5182. [PubMed: 7523307]
25. Stark ME, Szurszewski JH. Role of nitric oxide in gastrointestinal and hepatic function and disease. Gastroenterology 1992;103:1928–1949. [PubMed: 1333429]
26. Mashimo H, Goyal RK. Lessons from genetically engineered animal models IV. Nitric oxide synthase gene knockout mice. Am J Physiol Gastrointest Liver Physiol 1999;277:G745–G750.
27. Mungrue I, Husain M, Stewart DJ. The role of NOS in heart failure: lessons from murine genetic models. Heart Fail Rev 2002;7:407–422. [PubMed: 12379825]
28. Ny L, Persson K, Larsson B, Chan J, Weiss LM, Wittner M, Huang H, Tanowitz HB. Localization and activity of nitric oxide synthases in the gastrointestinal tract of *Trypanosoma cruzi*-infected mice. J Neuroimmunol 1999;99:27–35. [PubMed: 10496174]
29. Ny L, Alm P, Larsson B, Ekstrom P, Andersson KE. Nitric oxide pathway in cat esophagus: localization of nitric oxide synthase and functional effects. Am J Physiol Gastrointest Liver Physiol 1995;268:G59–G70.
30. Li E, Zhou P, Singer SM. Neuronal nitric oxide synthase is necessary for elimination of *Giardia lamblia* infections in mice. J Immunol 2006;176:516–521. [PubMed: 16365445]
31. Beck PL, Xavier R, Wong J, Ezedi I, Mashimo H, Mizoguchi A, Mizoguchi E, Bhan AK, Podolsky DK. Paradoxical roles of different nitric oxide synthase isoforms in colonic injury. Am J Physiol Gastrointest Liver Physiol 2004;286:G137–G147. [PubMed: 14665440]
32. Helmer KS, West SD, Shipley GL, Chang L, Cui Y, Mailman D, Mercer DW. Gastric nitric oxide synthase expression during endotoxemia: implications in mucosal defense in rats. Gastroenterology 2002;123:173–186. [PubMed: 12105846]

33. McCafferty DM, Mudgett JS, Swain MG, Kubes P. Inducible nitric oxide synthase plays a critical role in resolving intestinal inflammation. Gastroenterology 1997;112:1022–1027. [PubMed: 9041266]
34. Chandra M, Tanowitz HB, Petkova SB, Huang H, Weiss LM, Wittner M, Factor SM, Shtutin V, Jelicks LA, Chan J, Shirani J. Significance of inducible nitric oxide synthase in acute myocarditis caused by *Trypanosoma cruzi* (Tulahuen strain). Int J Parasitol 2002;32:897–905. [PubMed: 12062561]
35. Cummings KL, Tarleton RL. Inducible nitric oxide synthase is not essential for control of *Trypanosoma cruzi* infection in mice. Infect Immun 2004;72:4081–4089. [PubMed: 15213153]
36. Huang H, Chan J, Wittner M, Jelicks LA, Morris SA, Factor SM, Weiss LM, Braunstein VL, Bacchi CJ, Yarlett N, Chandra M, Shirani J, Tanowitz HB. Expression of cardiac cytokines and inducible form of nitric oxide synthase (NOS2) in *Trypanosoma cruzi*-infected mice. J Mol Cell Cardiol 1999;31:75–88. [PubMed: 10072717]
37. Huang H, Chan J, Wittner M, Weiss LM, Bacchi CJ, Yarlett N, Martinez M, Morris SM, Braunstein VL, Factor SA, Tanowitz HB. *Trypanosoma cruzi* infection induces myocardial nitric oxide synthase. Cardiovasc Pathol 1997;6:161–166.
38. Jelicks LA, Shirani J, Wittner M, Chandra M, Weiss LM, Factor SM, Bekirov I, Braunstein VL, Chan J, Huang H, Tanowitz HB. Application of cardiac gated magnetic resonance imaging in murine Chagas disease. Am J Trop Med Hyg 1999;61:207–214. [PubMed: 10463668]
39. James SL. Role of nitric oxide in parasitic infections. Microbiol Rev 1995;59:533–547. [PubMed: 8531884]
40. Nathan C, Shiloh MU. Reactive oxygen and nitrogen intermediates in the relationship between mammalian hosts and microbial pathogens. Proc Natl Acad Sci USA 2000;97:8841–8848. [PubMed: 10922044]
41. Bittencourt AL, Viera GO, Tavares HC, Moto E, Maguire J. Esophageal involvement in congenital Chagas' disease. Report of a case with megaesophagus. Am J Trop Med Hyg 1984;33:30–33. [PubMed: 6421181]
42. Da-Costa-Pinto EAL, Almeida EA, Figueiredo D, Bucaretchi F, Hessel G. Chagasic megaesophagus and megacolon diagnosed in childhood and probably caused by vertical transmission. Rev Inst Med Trop S Paulo 2001;43:227–230. [PubMed: 11558004]

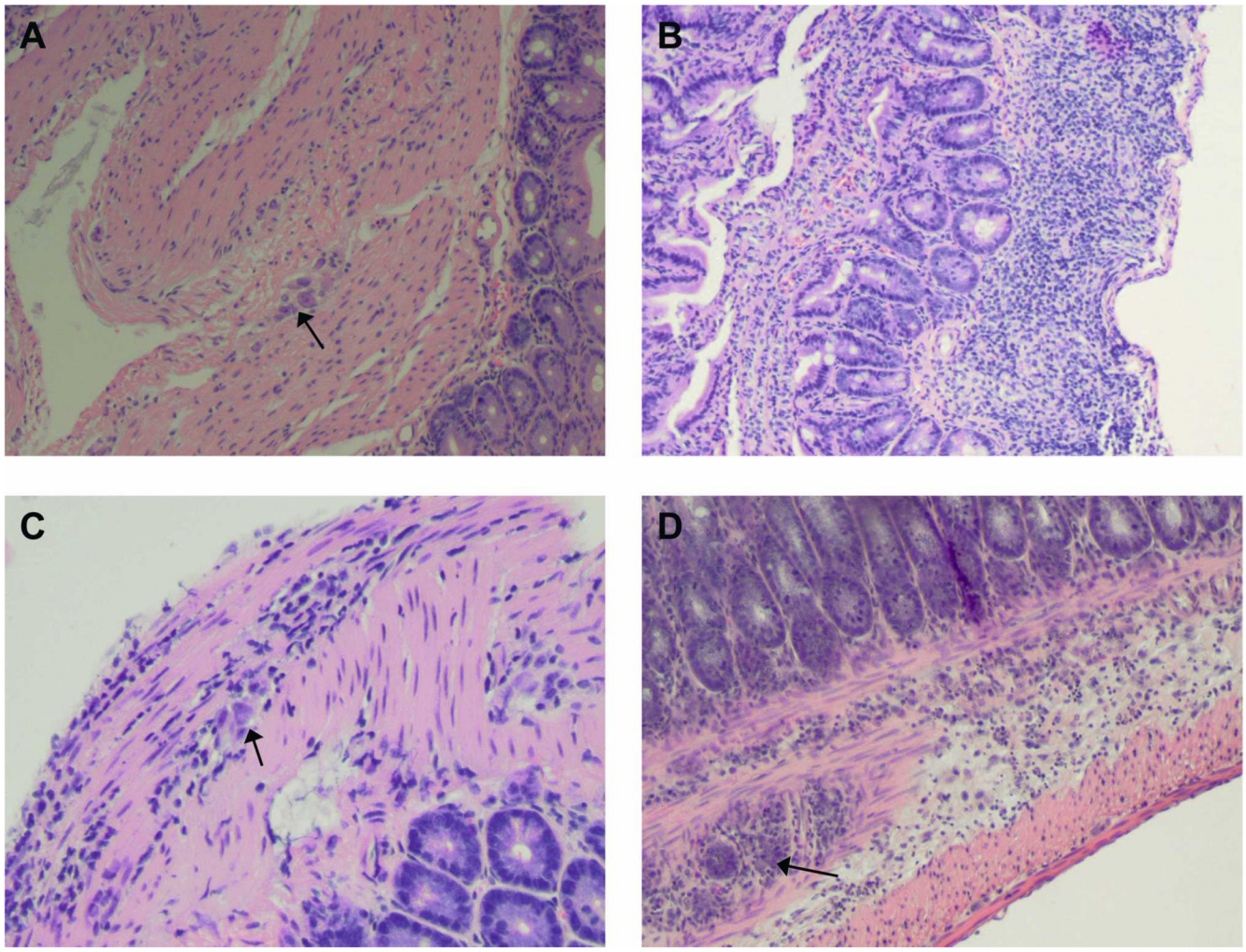

FIGURE 1.

Representative histology of colon obtained from infected mice. (**A**) Uninfected wild-type (WT) mouse. Note the normal ganglia (arrow, original magnification, 10×). (**B**) Infected NOS2 null mouse. Note the marked inflammatory response (original magnification, 10×). (**C**) Infected NOS2 null mouse. Note the ganglionitis (arrow, original magnification 20×). (**D**) Infected NOS2 null mouse. Note the marked inflammation and ganglionitis (arrow, original magnification, 10×). This figure appears in color at www.ajtmh.org.

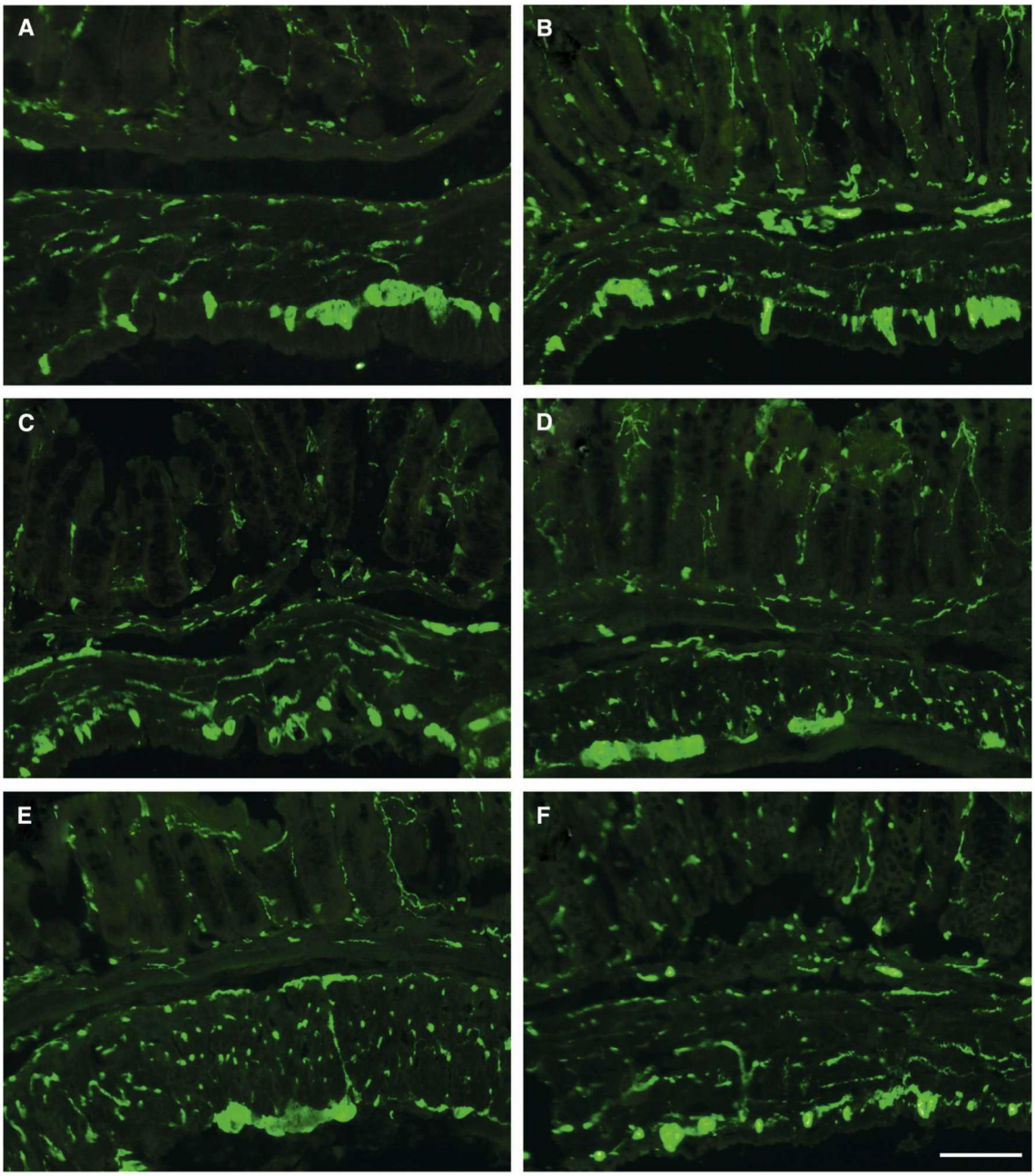

FIGURE 2.

Immunofluorescent images demonstrating protein gene product (PGP)-immunoreactivity in the intestinal wall of the mouse colon from (**A**) uninfected NOS1null, (**B**) infected NOS1 null, (**C**) uninfected NOS2 null, (**D**) infected NOS2 null, (**E**) uninfected wild-type (WT), and (**F**) infected WT. This figure appears in color at www.ajtmh.org.

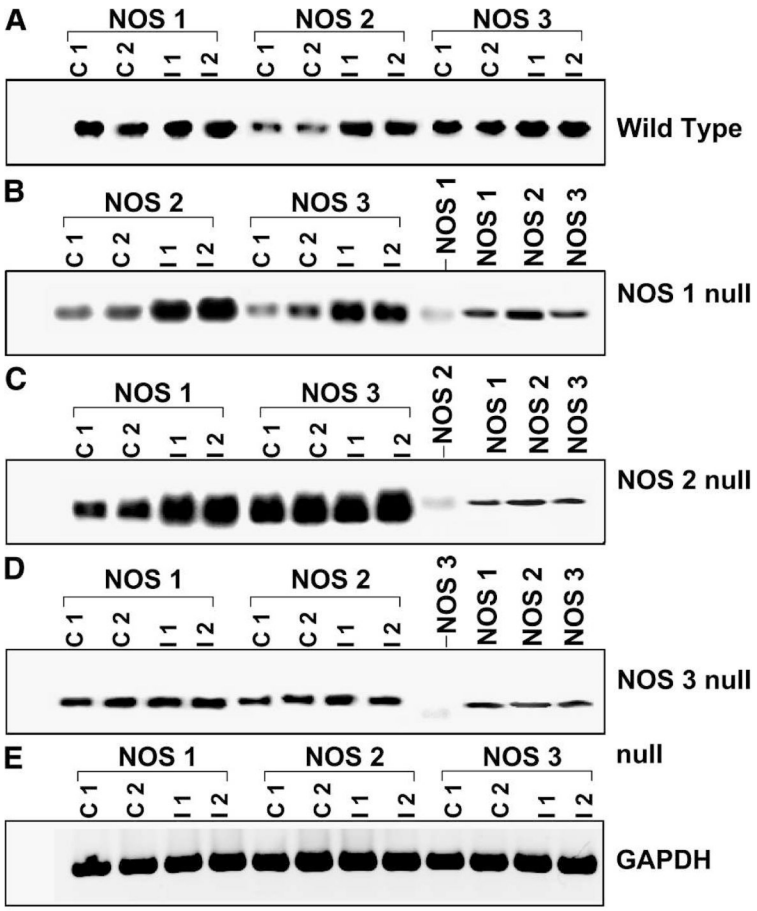

FIGURE 3.

Semi-quantitative reverse transcription-polymerase chain reaction (RT-PCR) for NOS isoforms in colon of wild-type (WT) and various NOS null mice. The top panel (**A**) shows various NOS isoform expression in WT control and infected mice. Representative gels of RT-PCR for NOS 2 and NOS 3 in NOS 1 null (**B**), NOS 1 and NOS 3 in NOS 2 null (**C**), and NOS 1 and NOS 2 in NOS 3 null (**D**), mouse colon infected with *T. cruzi*. Data from two independent control (C 1 and C 2) and infected (I 1 and I 2) samples from WT and each null mouse is shown. In panels (**B**), (**C**), and (**D**), the respective NOS null isoform was also amplified as a negative control. The right-hand side NOS 1, 2, and 3 are NOS positive controls, amplified from purified NOS cDNAs (as mentioned in Materials and Methods). Panel (e) shows GAPDH RT-PCR as an internal control, which remained the same in all NOS null mice regardless of infection status.

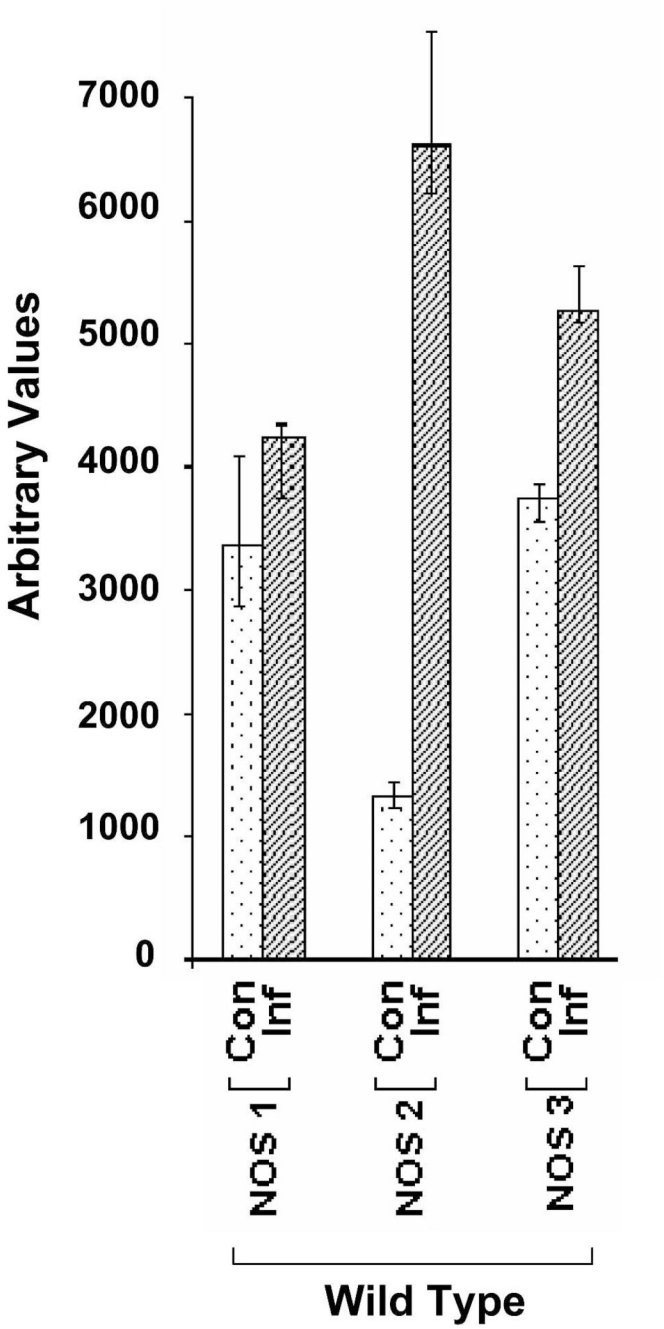

FIGURE 4.

The relative contribution of NOS isoforms in mouse colon in *T. cruzi* infection. Semi-quantitative reverse transcription-polymerase chain reaction (RT-PCR) data for NOS isoforms are presented graphically for wild-type (WT) infected mice. A significant over expression of both NOS2 and NOS3 isoforms was observed.

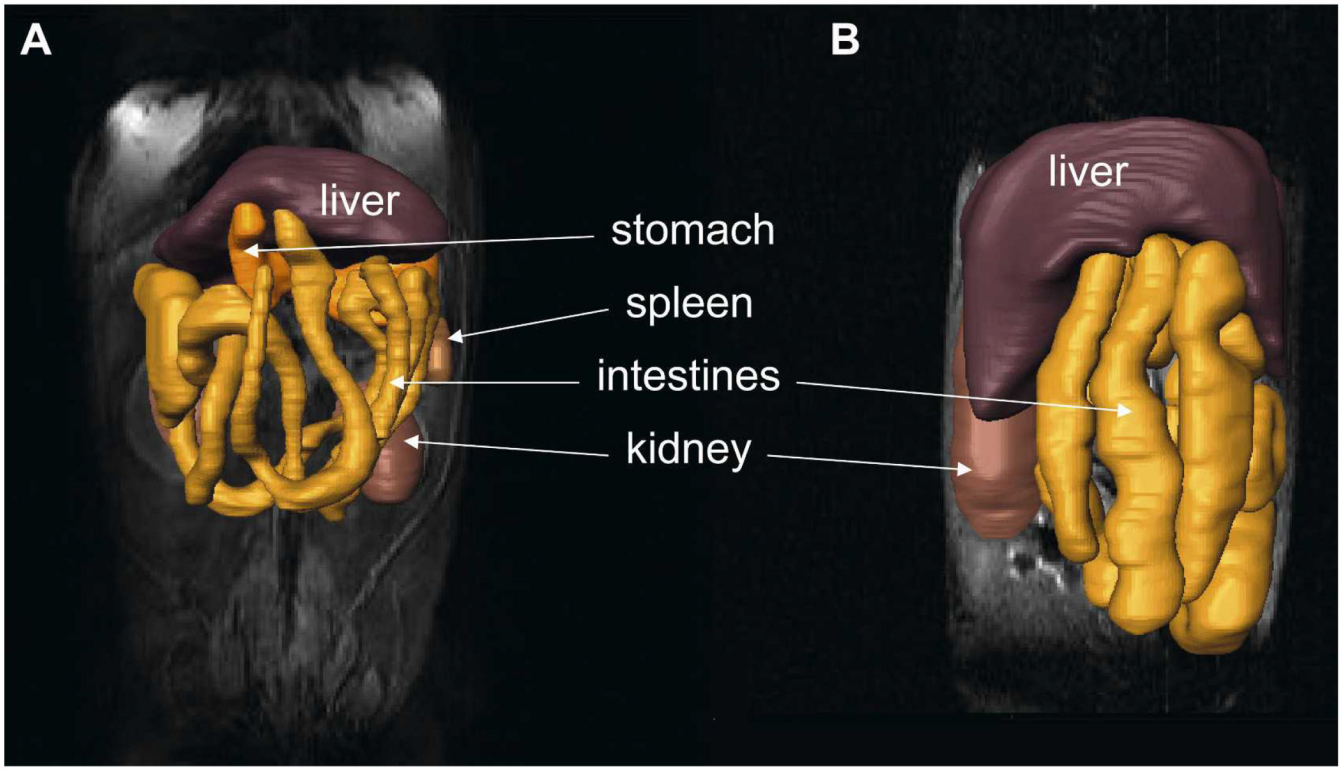

FIGURE 5.
Three-dimensional reconstructions of the gastrointestinal (GI) tract from magnetic resonance imaging (MRI) images of (**A**) an uninfected wild-type (WT) mouse and (**B**) an infected WT mouse. The reconstructions are overlaid on the original MRI images. Several organs are indicated. This figure appears in color at www.ajtmh.org.

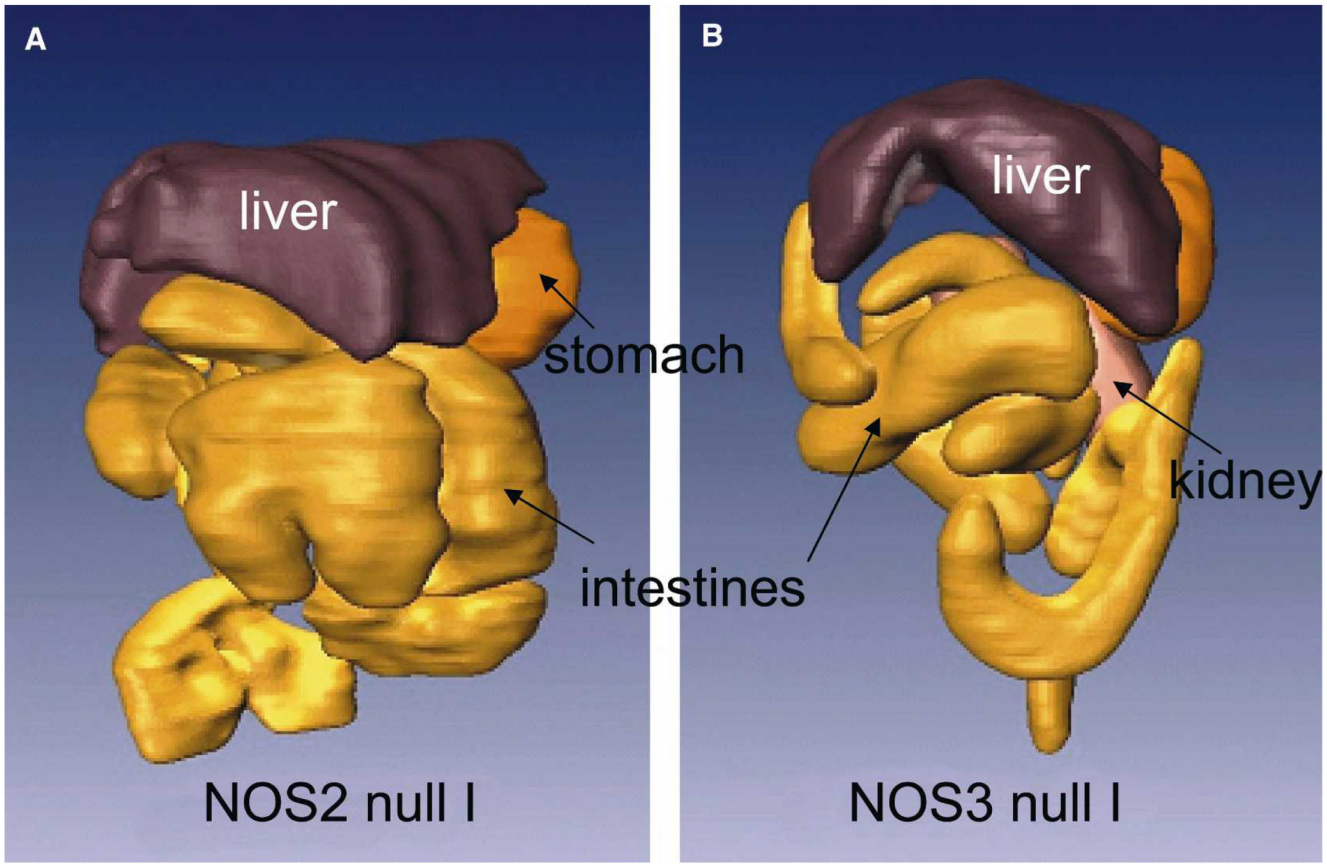

FIGURE 6.

Three-dimensional reconstructions of the gastrointestinal (GI) tract from magnetic resonance imaging (MRI) images of (**A**) an infected NOS2 null mouse and (**B**) an infected NOS3 null mouse. Several organs are indicated. This figure appears in color at www.ajtmh.org.

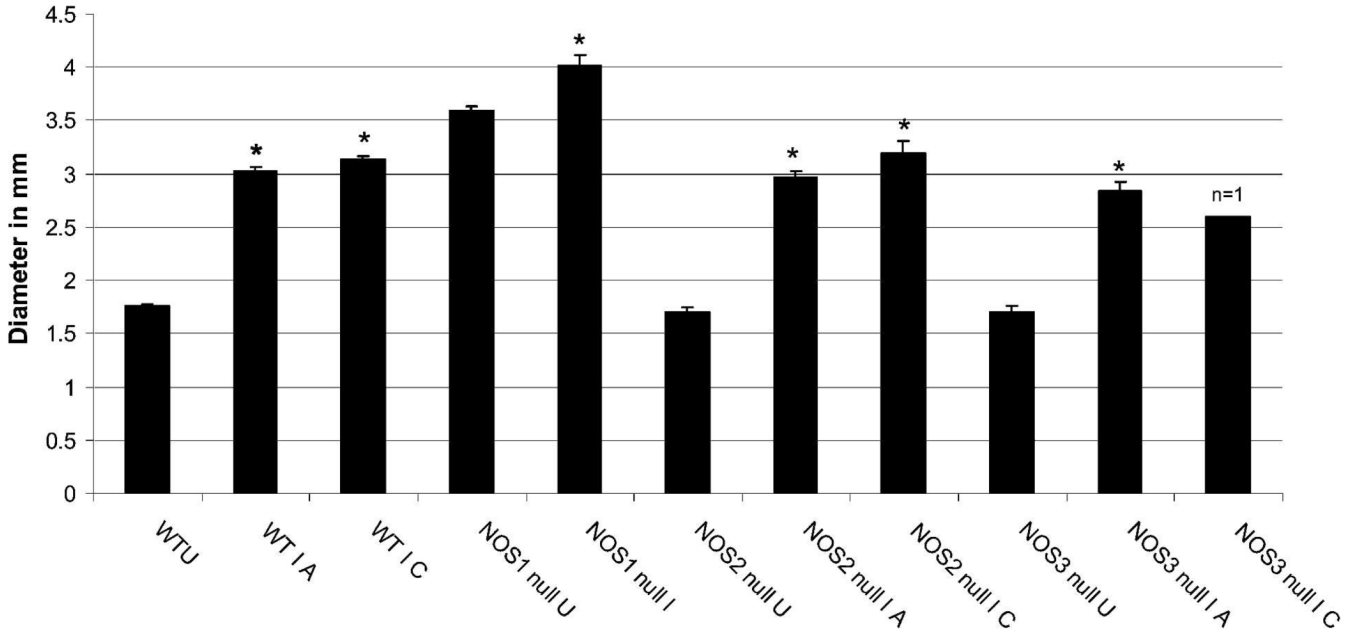

FIGURE 7.

Intestine lumen diameter measured at the region of the kidney in transverse magnetic resonance imaging (MRI) images. Lumen diameter was compared at the acute (A, 30 dpi) and chronic (C, 60 dpi) for all groups except NOS1 (no infected NOS1 null mice survived to the 60 days time point). Wild-type uninfected (WTU) is the average of 29 measurements (4 mice); WT I A (wild type infected, 30 dpi) is the average of 31 measurements (5 mice); WT I C (wild type infected, 60 dpi) is the average of 10 measurements (2 mice); NOS1 null U (NOS1 null uninfected) = 55 measurements (9 mice); NOS1 null I A (NOS1 null infected, 30 dpi) = 23 measurements (5 mice); NOS2 null U (NOS2 null uninfected) = 29 measurements (5 mice); NOS2 null I A (NOS2 null infected, 30 dpi) = 42 measurements (7 mice); NOS2 null I C (NOS2 null infected, 60 dpi) = 12 measurements (2 mice); NOS3 null U (NOS3 null uninfected) = 28 measurements (4 mice); NOS3 null I A (NOS3 null infected) = 18 measurements (3 mice); NOS3 null I C (NOS3 null infected) = 7 measurements (1 mouse). *Lumen diameter was significantly increased in all infected mouse groups compared with their respective uninfected groups (*t* test, $P < 0.001$ for WT, NOS2 null, and NOS3 null, and $P = 0.018$ for NOS2 null). The extent of increase in lumen diameter during acute versus chronic infection was not significantly different for the WT, NOS2 null, and NOS3 null mice.